Contributed paper

OPTO-ELECTRONICS REVIEW **13**(3), 213–220

Investigation of structural, optical and lasing properties of YAG:Yb single crystals

M. ŚWIRKOWICZ[1*], M. SKÓRCZAKOWSKI[2], J. JABCZYŃSKI[2], A. BAJOR[1], E. TYMICKI[1], B. KACZMAREK[1], and T. ŁUKASIEWICZ[1]

[1] Institute of Electronic Materials Technology, 133 Wólczyńska Str., 01-919 Warsaw, Poland
[2] Institute of Optoelectronics, Military University of Technology, 2 Kaliskiego Str., 00-908 Warsaw, Poland

Single crystals of yttrium aluminium garnet (YAG) doped with ytterbium ions of up to 30 at.% were grown by the Czochralski method. Using the growth rate from 1 to 3 mm/h, and the rotation rate from 15 to 30 rpm, single crystals with diameters of up to 22 mm and lengths up to 85 mm were obtained. Using the inductively coupled plasma – optical emission spectroscopy (ICP-OES) method, Yb distribution coefficient was determined to be equal to 1.10±0.02. The following methods: optical absorption spectroscopy, plane and circular polariscope, electron probe microanalysis (EPMA) to determine the radial distribution of Yb ions, X-ray diffraction methods to determine the lattice constant were used. Etch pit density distribution and lasing properties were also investigated. Samples of YAG:Yb crystals with Yb ions contents of 3, 5, 7, and 10 at.% were pumped by 940 nm laser diode for their lasing properties. The best lasing slope efficiency of 40% with respect to the absorbed pump power was achieved at 5 at.% Yb content. The lowest threshold of 2.5 W of the absorbed pump power was observed, however, for a 7 at.% Yb doped sample in quasi hemispherical resonator configuration. These investigations have been found to be in good agreement with polariscopic observations, showing a certain decrease in optical homogeneity with increase in Yb content.

Keywords: Czochralski method, YAG: Yb, growth from melt, oxides, optical and lasing properties.

1. Introduction

The first announcement on YAG:Yb lasers pumped with flash-lamps appeared in 1965 [1]. However, this work was abandoned in consequence of certain problems associated with adequate pumping band in case of Yb ions, in comparison with other rare earth dopants (especially that of Nd). When high power laser diodes became available, they could replace flash or arc pump-lamps. This resulted in diode-pumped solid-state lasers (DPSSL), being currently most perspective in laser technique. Firstly, AlGaAs laser diodes were used mainly for materials doped with neodymium (YAG:Nd, YVO_4:Nd, $LiYF_4$:Nd) [2]. When commercial high power InGaAs diode pumps appeared, it stimulated the intensive works on Yb lasers, and also on YAG: Yb [2–5].

One should notice several advantages of YAG:Yb crystal over commonly used YAG: Nd [2,6], like closeness of their absorption (941 nm) and emission (1029 nm) peaks, broad absorption band (18 nm), long radiative lifetime (0.95 ms), and very low fractional heat generation (< 11%). Also, no absorption and upconversion losses are observed in this material. As a host material, YAG is specially adequate for Yb doping: it has high thermal conductivity and especially similar ionic radius of Y to substitute [7].

Due to possibility of doping to a high level and low quenching, the material could be used in power lasers and in microlasers (with high Yb concentration – above 10%).

In this work single crystals of YAG doped with ytterbium up to 30 at.% were grown and their optical and lasing properties were investigated.

2. Experimental procedure

2.1. Growth of single crystals

All the crystals were grown by the Czochralski method from the melt using the Oxypuller 05-03 equipment made in France by Cyberstar. The inductive heating with Hüttinger generator was used.

The charge material was prepared on the basis of a 4.5 N grade Y_2O_3, Al_2O_3 and Yb_2O_3 oxides. $Y_3Al_5O_{12}$ and $Yb_3Al_5O_{12}$ compounds were obtained, and any charge with the appropriate dopant level (up to 30 at.% Yb) was achieved as a mixture of these two garnets. The quantity adequate to fill a 50-mm diameter crucible was isostatically pressed and next melted (normally in two runs).

The thermal system consists of a 50-mm diameter and 50-mm high iridium crucible, embedded in Zircar zirconia grog, a passive iridium afterheater placed on the grog around the top part of the crucible, as well as alumina heat shields around the afterheater itself.

*e-mail: swirko_m@itme.edu.pl

The Cyberstar program prepared on the basis of a Test Point with melt level lowering compensation taken into account, has been used to control the whole growth runs. The system is equipped in Sartorius balance weighing the growing crystal (the base of ADC – automatic diameter control) and additionally in the crucible translation unit.

The growing atmosphere was either a pure nitrogen, or nitrogen with a certain amount of oxygen (0.2–0.5 vol%). The following conditions of the growth process have been applied: growth rate 1–3 mm/h; rotation rate 15–30 rpm; cooling after growth – at least 24 h.

The following crystals were obtained: undoped, 1, 1.5, 2, 3, 5, 7, 10, 15, 20, 25, and 30 Yb at.% doped, respectively. All the crystals were <111> oriented, 17–22 mm in diameter and up to 85 mm long. When they were grown in pure nitrogen atmosphere, their colour was changing with an increase in ytterbium content from colourless to pale blue. When using nitrogen with admixture of oxygen, the crystals were always colourless. Some of the crystals are shown in Fig. 1. A certain increase in blue coloration with increase in the Yb content can be observed.

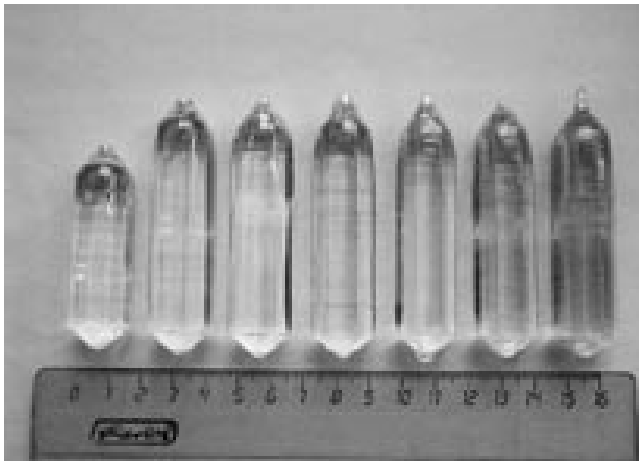

Fig. 1. YAG:Yb single crystals (from left to right 1, 1.5, 2, 3, 5, 7, and 10 at.%; the scale is in cm).

2.2. Preparation of samples

The obtained single crystal boules were annealed in the air at 1100°C for 1 h, and then slowly cooled down to room temperature. Samples were prepared for distribution of ytterbium and lattice constant evaluation, and for optical and laser measurements.

According to theoretical predictions and to some initial experiments, in case of investigation of lasing properties the samples should be shaped as thin discs (in our case 6 mm in diameter and 2–3 mm thick). Such shape ensures a good heat conduction and cooling, and minimizes also transversal thermal effects leading to transversal temperature gradients, and hence, to a significant thermal lensing.

All discs have been polished to achieve good parallelism of the both faces, and then dielectrically coated. One face of the disc was transparent for pumping radiation (approximately 85% transmittance at 940 nm), while near the lasing wavelength (1030–1130 nm) it became totally reflective. The second face with antireflection coating was optimised for the lasing wavelength.

3. Results

3.1. Polariscopic observations

The both polariscopes, i.e., plain, comprising a pair of two plane polarizers, and circular, comprising also two quarterwave plates, are simple and convenient tools for quick estimation of magnitudes of the so-called residual stresses [8,9] and also symmetry of their distribution. If the sample is being placed between two crossed polarizers in the plane polariscope, one can usually see dark lines on the sample bright area. These lines are called the isoclinics, and are associated with the principal stress directions. Sometimes, another dark lines, called isochromatics of the even order of retardation, and associated with the appropriate magnitudes of the residual stresses, may also appear in the polariscopic image. While the polarizers are being paralleled, the isoclinics disappear, and new dark lines, i.e., the isochromatics of the odd order of retardation may appear instead.

In the circular polariscope no isoclinics do appear at all. It may be sometimes convenient, especially in highly stressed samples, when the isoclinics and the isochromatics may overlap each other, to use this polariscopic configuration for a quick assessment of magnitudes of the residual stresses. In such a case, when the quarterwave plates are being crossed, one can observe only isochromatics of the even order of retardation, whereas isochromatics of the odd order of retardation may appear in the parallel quarterwave configuration.

It is important to study the residual birefringence, associated with the residual stresses, because it always degrades, to a smaller or to a greater extent, parameters of practically all optical devices (e.g. Ref. 10), including lasers. Therefore, it is advisable to select those parts of crystals which are free from excessive residual stresses, as well as macroscopic defects, easily visible in polariscopic investigations.

It has been found that the stresses were mostly concentrated in and around the central core region, and this observation was also consistent with experiments, e.g. that of Koechner and Rice [11]. The perimeters of the crystals were almost free from residual stresses for low doping levels, with an exception of those peripheral parts, being close to the "corners of the hexagon", i.e., the figure resembling the crystal's cross-section. A noticeable increase in optical inhomogeneity with doping can be observed in Fig. 2. A more deformed isoclinic cross, as well as a clear movement of the black isochromatic (of the 1st order of retardation, situated close to the core) from the core towards the periphery of the boules, can be observed in this figure with the increase in Yb content. This also means that the maximum of

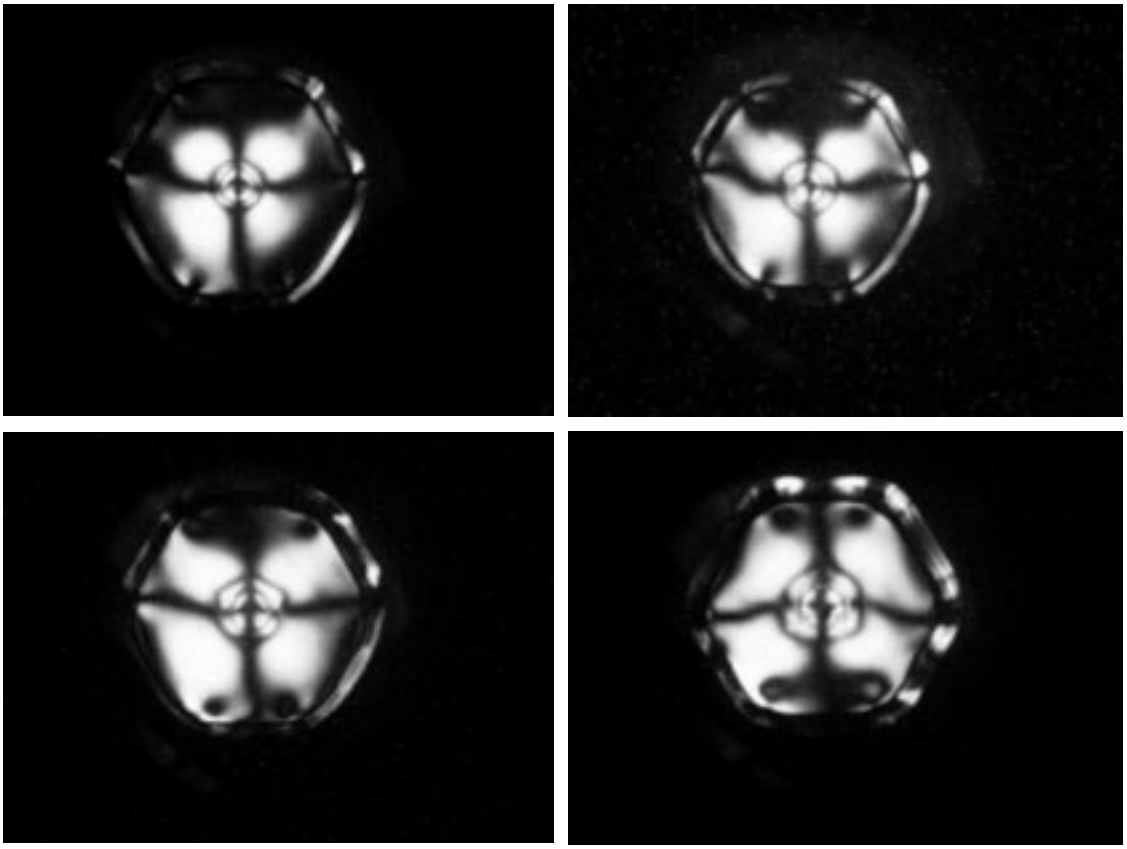

Fig. 2. Plane polariscope pictures of YAG:Yb crystals: the Yb concentration is (from left to right and from top to bottom) 7, 15, 20, and 30 at.%, respectively.

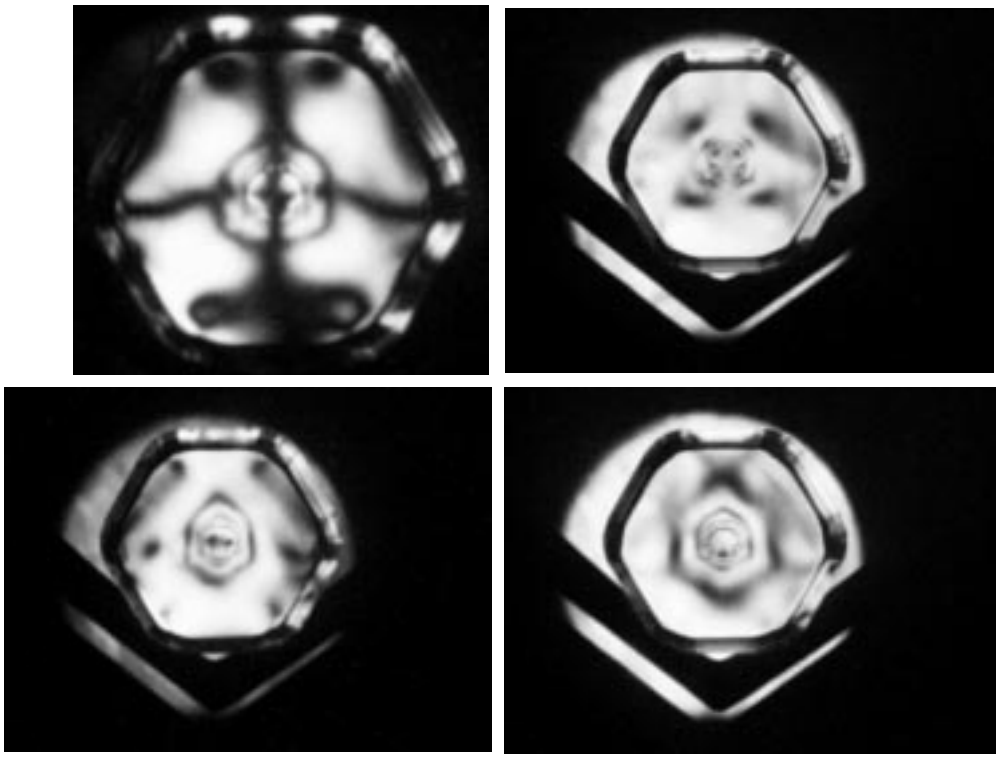

Fig. 3. Plane polariscope pictures in crossed polarizers configuration (top left), and in parallel polarizers configuration (top right), as well as circular polariscope pictures in crossed quarter wave plates configuration (bottom left), and in parallel quarter wave plates configuration (bottom right), respectively, in YAG doped with 30% of Yb.

the residual stresses (birefringence) is constantly shifting away from the core when the Yb content increases. Fortunately, also in the case of highly doped crystals, these investigations have neither revealed very large residual stresses, nor any additional macroscopic defects, but in the vicinity of the core region itself (Fig. 3). In this figure, a considerable deformation of arms of the isoclinic cross can be seen only at the perimeter area, and this implies also a certain departure from radial symmetry of the residual stress distribution, which, however, is typical for o oriented crystals. Hopefully, the above mentioned isochromatic (the zero-order of retardation isochromatics are situated exactly at the perimeter of the crystal and the core itself – the difference of the principal radial and tangential residual stresses changes its sign in the core region), as well as the 1/2 order of the retardation isochromatics, evidenced on circular polariscope pictures in Fig. 3, are situated so close to the core, and also so faraway from the perimeter, that one could always select adequate parts of crystals, faraway from the core and from the perimeter regions, respectively, suitable for laser applications.

3.2. Etch pit density distribution (EPD)

The EPD was measured in two types of wafers: cut out from the cone and from the tail parts of crystals, respectively. The pits were revealed by etching the wafers in 85% orthophosphoric acid at 240°C for 20 min.

The observations were made under microscope and computer-controlled counting of EPD in all the crystals with different Yb content has been performed. Some of our results for YAG: 20 at.% of Yb have been presented below. The EPD images were recorded in 6 different points, beginning at the centre, and ending at the periphery of each wafer. For example, in Fig. 4 one can see a set of such images in one of the wafers, while a plot of EPD distribution along the crystal radius has been depicted in Fig. 5 for both types of wafers.

An increase in EPD with the radius is basically consistent with theory [8,12], and practice [8,13] of generation of dislocations in Czochralski-grown crystals. Nearly all theories predict that EPD should be constantly increasing from the centre to the periphery. They also do believe that the EPD should be increasing from top to bottom. We have, however, observed another phenomenon, namely of a certain decrease in EPD at the end part of this crystal. Moreover, the EPD was to a certain extent inconsistent with polariscopic observations reported above. Providing that EPD is proportional to the real density of dislocations, which are surrounded by local stress fields, one should expect rather a larger such densities in the centre, as well as in the regions situated nearby to those "corners of the hexagon". It is believed that this discrepancy can be attributed to existence of the core region itself, which is not included in the models, as well as to a very large thermal conductivity of the YAGs, causing also a certain departure from classical models. For example, it has been anticipated (Gałązka, Ref. 14) and proved experimentally (Bajor *et al.*, Ref. 15) that the stresses in oxide crystals may not necessarily be largest at the boule's tail. However, it seems that

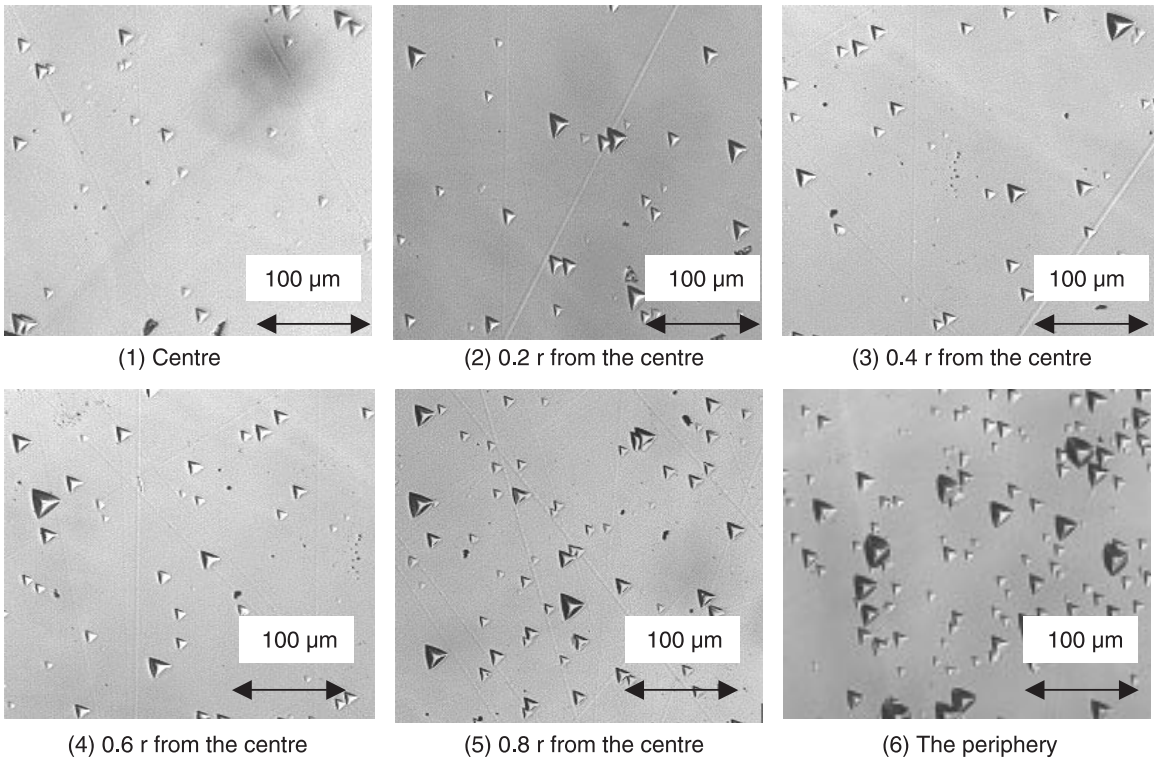

Fig. 4. Etch pit distribution along wafer radius (the wafer cut out from the end part of the boule).

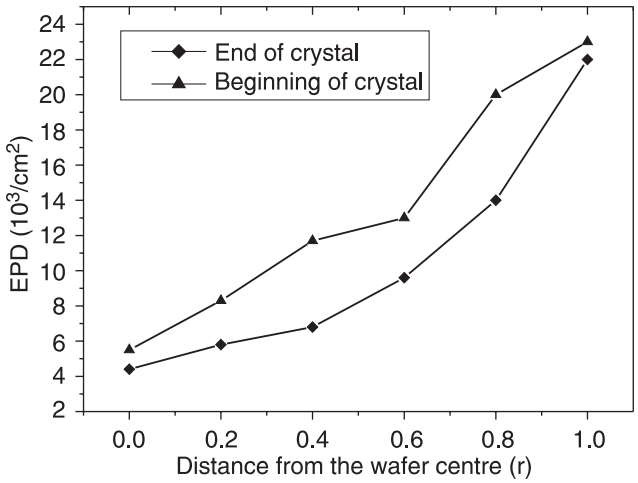

Fig. 5. Radial distribution of etch pit density for YAG: 20 at.% Yb single crystal (▲ – beginning of the boule, ◆ – end of the boule).

by combining the two methods, i.e., polariscopic and EPD, one is always able to select the appropriate crystal parts, usually located just between the core and the perimeter, to provide the most suitable structures for laser applications.

3.3. Yb distribution, optical absorption and X-ray diffraction measurements

Homogeneity of Yb distribution and the absorption coefficient itself, are another crucial factors in laser operation.

In order to determine the distribution coefficient of Yb in YAG, the samples were cut out from the top and bottom parts of the boules, grown from the charge materials of definite compositions. The Yb content was measured using the inductively coupled plasma-optical emission spectroscopy (ICP-OES) method. According to our results (for Yb content up to 15 at.%), this coefficient was equal to $k_{Yb} = 1.10 \pm 0.02$ and was very close to that obtained elsewhere [16].

The lattice constant of YAG:Yb was investigated at room temperature by means of the precise X-ray powder diffraction method using a Siemens D500 diffractometer with CuK_α radiation and high-resolution Si: Li semiconductor detector. The diffraction patterns were measured in the /2 scanning mode in the angle range of 50–120° with a step of 0.02° and counting time of 10 sec. The lattice constant was measured as a function of doping concentration of up to 30 at.% of Yb. It was found that the lattice constant decreases linearly with the increase in Yb content (Fig. 6). This could be anticipated earlier, since the ionic radius of the Yb ion is smaller than that of Y.

We have also measured radial distribution of Yb using EPMA (equipment CAMECA SX 100). The measurements were performed in crystals with 3, 5, and 10 at.% of Yb. This distribution was found to be very homogenous with an exception for parts of the crystals close to their perimeters (Fig. 7). And this is also another indication that the crystalline areas close to the perimeters should rather be not used in laser experiments.

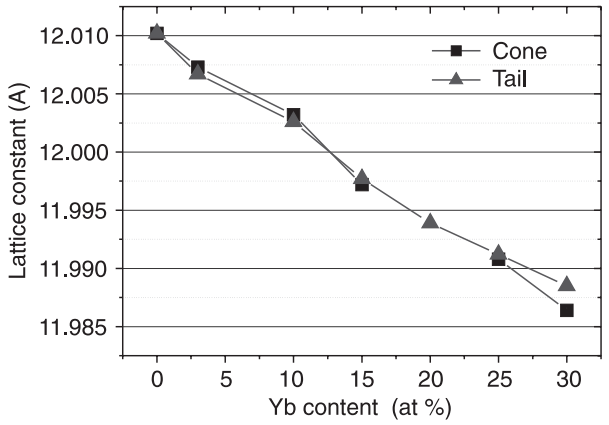

Fig. 6. Dependence of lattice constant on Yb content.

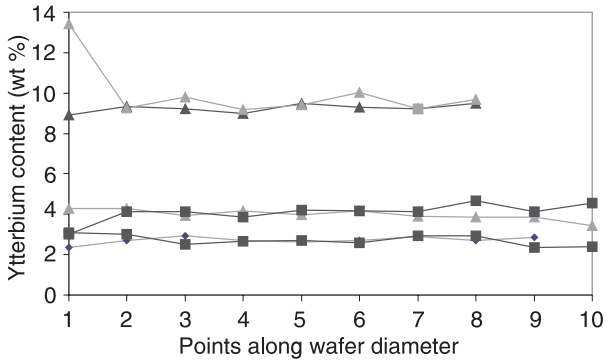

Fig. 7. Radial distribution of ytterbium in YAG:Yb single crystal wafers for 3, 5 and 10 at.% Yb, cut from the tail (square) and the cone (triangle) parts, respectively.

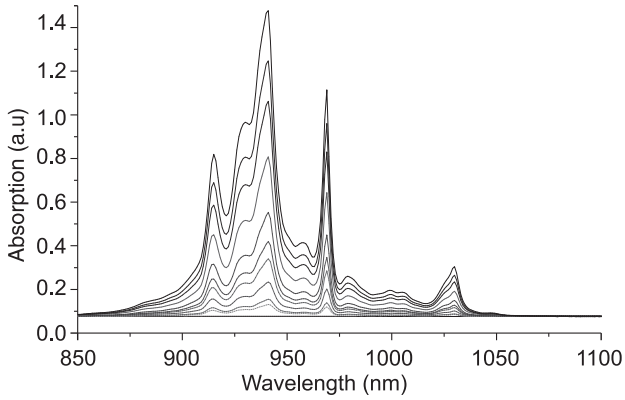

Fig. 8. The optical absorption in dependence on Yb content (from bottom to top: undoped, 1, 1.5, 3, 5, 7, 10, 15, 20, 25, and 30 at.%).

The optical absorption was also measured as a function of Yb content up to 30 at.%, using UV-VIS-NIR VARIAN spectrophotometer of CARRY 500 type. As shown in Fig. 8, the absorption coefficient depends linearly on the Yb content. The Yb absorption peak observed at 940 nm, associated with $^2F_{7/2} \rightarrow {}^2F_{5/2}$ transition is clearly visible. Since the crystals were grown in nitrogen-oxygen atmosphere, or were afterward annealed in the air, neither additional absorption bands due to Yb^{2+} ions, nor colour centres were observed.

3.4. Investigation of lasing properties

All measurements reported above have revealed that when cutting off a structure for laser application, one should be especially aware of the core and the nearby regions of the crystal. However, also the regions situated close to the perimeter were also found unsuitable for laser applications. Thanks to all these results, we have been cutting out our lasing structures from selected parts of the boules. Lasing properties were investigated in two configurations, namely pulsed and (quasi)continuous.

Pulsed mode operation. The first experiment has been carried out in the pulse regime using pulsed diode driver of SDL 928-10 type, suitable for working with pump pulses as long as 1.1 ms. The driver was triggered with a minimal repetition rate of 14 Hz in order to decrease thermal loading of the crystal as far as possible, because the crystal was freely mounted in a typical mirror holder and was not cooled. Although an average power absorbed in the crystal was only 150 mW, a significant temperature rise was observed, resulting in decreasing the output power by about 10% during a few minutes of the laser operation. The slope efficiency exceeding 50% has been obtained for the sample with 5 at.% of Yb in a plane-concave 4.5 cm long cavity (Fig. 9). The extrapolated threshold pump energy was found to be as low as 3.4 mJ, equivalent to about 3 W of continuous wave (CW) threshold, when the laser had not been subjected to thermal loading. For the same resonator configuration, in CW mode the threshold power was approximately equal to 4.7 W, and the slope efficiency was approaching 40% (Fig. 10). This was caused by temperature increase when the laser was CW operated.

CW mode operation. Having obtained satisfactory results in the pulsed mode, we have also checked the CW behaviour. However, the structures had to be effectively cooled, and, therefore, a special miniature copper heatsinks, on both structure faces were designed. The heatsinks had 1.5 mm dia. holes in their centers to provide the optical path for pumping and laser beams. Their surfaces were polished and no additional intermediate heat-conducting media were applied. However, to increase cooling of the structures, also a small flow of water, cooled down to about 12°C, was applied.

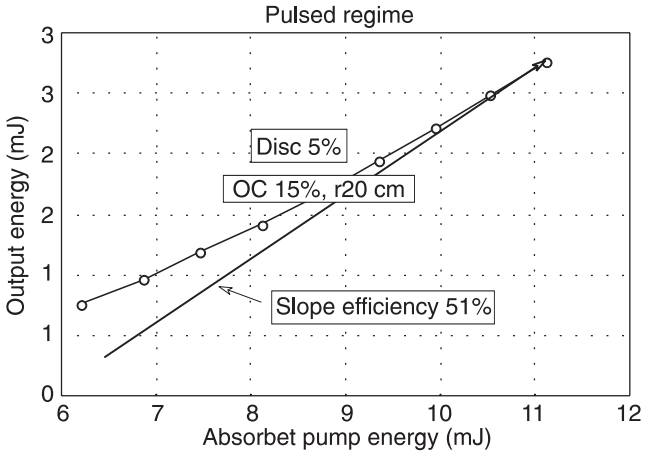

Fig. 9. YAG:Yb thin disc laser output energy versus absorbed pump energy in low thermal loading regime (low repetition rate pulsed mode). The output coupler was 20 cm concave mirror with 15% of transmittance.

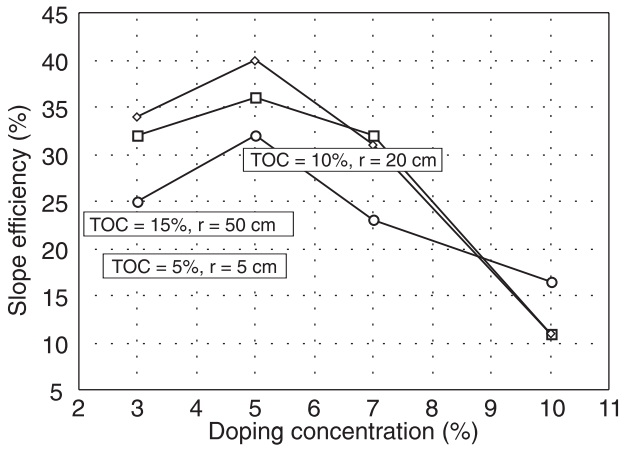

Fig. 10. CW YAG:Yb thin disc laser slope efficiency versus Yb concentration. Each plot concerns different resonator geometry and the output coupler transmittance.

Four resonator configurations utilizing six different output couplers have been used during these investigations:

(a) the set of concave mirrors having the radius of curvature of 50 cm and the following transmittances: 1,3%, 5%, or 15%,
(b) the set of concave mirrors having the radius of curvature of 20 cm and the following transmittances: 10% or 15%,
(c) flat mirror with a 10% transmittance,
(d) concave mirror with a 5 cm radius curvature and 5% transmittance.

Each resonator was fixed to be 4.5 cm long, which also resulted in its stable operation providing that thermal lensing was not taken into account. However, no significant thermal lensing was evidenced here, even for the maximum pumping power, because no dramatic fall in the output power with the increase in pumping power has been observed. This favourable result confirms our observation that thermal loading in YAG:Yb crystal is relatively low, being also the consequence of extremely low quantum defect, as well as high quantum efficiency.

A 25-W laser diode was used for pumping. The pumping power was delivered into the lasing structure through a 1.5 m long, 400 μm diameter flexible multimode fibre. For this reason, the pumping power delivered directly to the structure was only about 15 W at the maximum current of 42 A. Depending on the sample length and concentration of Yb ions, the optical power transmitted through the structures varied from 1 W (for 10% Yb doping), up to 5 W (for 3% doping). Unlike in linear transmission, an abrupt increase in transmission was also observed when the crystals were strongly pumped. Therefore, one can say that the pumping intensity inside the crystal was actually in the

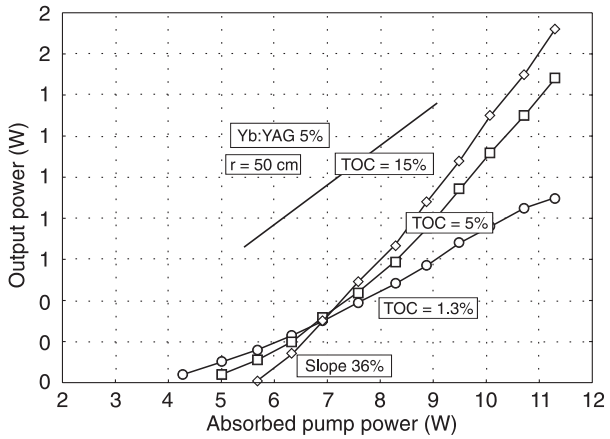

Fig. 11. YAG:Yb thin disc laser output power versus absorbed pump power in CW regime for the set of the output couplers described in the text as (a). All the output couplers were concave with the radius of curvature equals 50 cm.

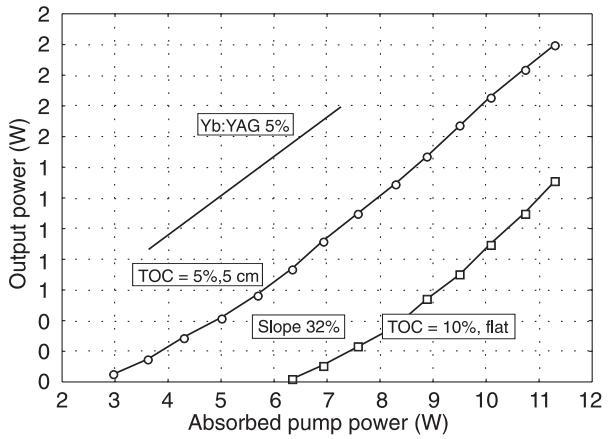

Fig. 12. YAG:Yb thin disc laser output power versus absorbed pump power in CW regime for both output couplers described in the text as (c) and (d).

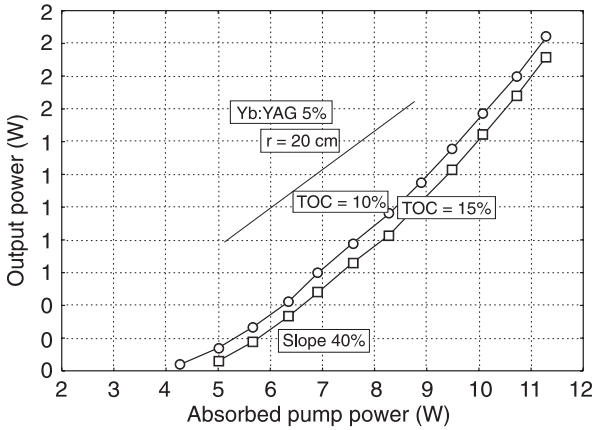

Fig. 13. YAG:Yb thin disc laser output power versus absorbed pump power in CW regime for the set of the output couplers described in the text as (b). All the output couplers were concave with the radius of curvature equals 20 cm.

range of the saturation intensity of absorption. The lasers worked stably, especially for samples with lower doping.

The pumping laser diode was thermoelectrically cooled, and the optimal operating temperature was experimentally matched. Unfortunately, it was not possible to keep up this optimal temperature in all cases because of insufficient power of the thermoelectric cooler driver. Therefore we have changed the laser operating conditions, decreasing the average pump power by a factor of 0.5. The laser was supplied by 50-ms long light pulses repeated with a frequency of 10 Hz. Such pumping regime from physical point of view fulfils the (quasi) CW mode principles of operation. The delay time between the beginning of the pumping pulse and the moment when the initial laser relaxation oscillations begins, was only 0.2 ms, which was 0.4% of the pumping pulse width.

All structures were examined in the above mentioned resonator configurations to obtain the optimal slope efficiency. This specific parameter, seems to be most suitable for characterising lasing properties of the investigated YAG:Yb samples. As a rule, YAG:Yb laser works efficiently at high threshold due to its quasi three-level scheme. In Fig. 11, one can see dependence of the slope efficiency on doping level for some selected resonator configurations, for which the efficiency has been found to be optimal. From this it can be seen that the optimal Yb content was found to be equal to 5% for the pumping conditions we have applied. And for this Yb content, the slope efficiency has also been found to be extremely high for all the above mentioned resonator geometries.

In Figs. 12 and 13, the results of laser output power obtained for 5%-doped samples have been presented for all the resonator geometries. The pumping power and the output power values have been recalculated for the case of the CW regime. The extreme slope efficiency of 40% was achieved when the 20-cm concave mirror was used. For the both transmittances, i.e., for 10% and 15%, the results were almost the same.

4. Conclusions

In this paper we have demonstrated a series of Czochralski-grown YAG crystals doped with different concentrations of Yb up to 30 at.%. By means of optical polariscopy it has been evidenced that the crystals were free from macroscopic defects (excluding the central core region itself) and also from excessive residual stresses. However, a slight increase in optical inhomogeneity with the increase in Yb content was observed, and this was to a certain extent consistent with lasing properties of the crystals, having their optimum at value of 5 at.% Yb content.

Coloration of YAG:Yb crystals depends on the growth atmosphere. The crystals were blue when grown in pure nitrogen, and became colourless while grown in the mixture of nitrogen and oxygen. The blue colour can be easily removed by annealing the crystals in the air at 1100°C for 1 h. The absorption bands connected with the colour centres, usually seen near 380 and 640 nm (Xu *et al.*, Ref. 17) were not clearly observable.

The distribution coefficient of Yb in YAG was determined to be exactly: k_{Yb} = 1.10 ±0.02. Radial distribution of Yb was found to be very homogenous, except for the peripheral regions, and this was also another indication for that regions to be excluded from laser applications. It was also found that the lattice constant of YAG:Yb decreases linearly with increase of the Yb content. The EPD depends mainly on growth conditions and changes from 4.4×10^3 near the centre of a wafer to a 2.2×10^4 at periphery.

Thanks to these investigations we were able to select adequate parts of the crystals, potentially most suitable for laser applications. Therefore we could observe a good optical and structural properties of our lasing structures, evidenced by their lasing parameters. The obtained results (slope efficiency, output power) are comparable with that reported by Giesen *et al*. [18] and Kasamatsu *et al*. [19]. It should be emphasized that our results have been obtained at temperatures close to the room temperature.

Acknowledgements

This work has been supported by the Polish Ministry of Scientific Research and Information Technology (Grant No. 7 T11B 002 21). We would like to express our gratitude thanks to Dr R. Diduszko, Dr R. Jakiela, A. Karas and E. Jurkiewicz-Wegner for helping us in making structural and optical measurements.

References

1. L.F. Johnson, J.E. Geusic, and L.G. Van Uitert, "Coherent oscillations from Tm^{3+}, Ho^{3+}, Yb^{3+} and Er^{3+} ions in yttrium aluminum garnet", *Appl. Phys Lett.* **7**, 127–129 (1965).
2. W.F. Krupke, "New laser materials for diode pumped solid state lasers", *Current Opinion in Solid State and Materials Science* **4**, 197–201 (1999).
3. V.I. Chani, A. Yoshikawa, Y. Kuwano, K. Inaba, K. Omote, and T. Fukuda, "Preparation and characterization of Yb: $Y_3Al_5O_{12}$ fiber crystals", *Mater. Res. Bull.* **35**, 1615–1624 (2000).
4. P. Yang, P. Deng, J. Xu, and Z. Yin, "Growth of high-quality single crystal of 30 at.% Yb: YAG and its laser performance", *J. Cryst. Growth* **216**, 348–351 (2000).
5. P. Yang, P. Deng, Z. Yin, and Y. Tian, "The growth defects in Czochralski-grown Yb: YAG crystal", *J. Cryst. Growth* **218**, 87–92 (2000).
6. D.S. Sumida, A.A. Betin, H. Bruesselbach, R.B, Matthews, R. Reeder, and M.S. Mangir, "Diode-pumped Yb: YAG catches up with Nd: YAG", *Laser Focus World*, 63–67 (1999).
7. R.D. Shannon, "Revised effective ionic radii and systematic studies of interatomic distances in halides and chalcogenides", *Acta Cryst.* **A32**, 751–767 (1976).
8. V.L. Indenbom, "Ein Beitrag zur Entestchung von Spannungen und Versetzungen beim Kristallwachstum", *Krist. Tech.* **14**, 493–507 (1979).
9. V.L. Indenbom and V.B. Osvenskii, "Theoretical and experimental studies of generation of stress and dislocations in growing crystals", *Growth of Crystals* **13**, 279–290 (1986).
10. D.S. Kliger, J.W. Lewis, and C.E. Randall, *Polarized Light in Optics and Spectroscopy*, Academic Press, New York, 1990.
11. W. Koechner and D.K. Rice, "Effect of birefringence on the performance of linearly polarized YAG:Nd lasers", *IEEE J. Quant. Electron.* **QE6**, 557–566 (1970).
12. A.S. Jordan, A.R. Neida, and R. Caruso, "The theoretical and experimental fundamentals of decreasing dislocations in melt grown GaAs and InP", *J. Cryst. Growth* **76**, 243–262 (1986).
13. R.T. Chen and D.E. Holmes, "Dislocation studies in 3-inch diameter liquid encapsulated Czochralski GaAs", *J. Cryst. Growth* **61**, 111–124 (1983).
14. Z. Gałązka, "Analysis of thermal shock during rapid crystal extraction from melts", *Cryst. Res. Technol.* **34**, 635–640 (1999).
15. A.L. Bajor and Z. Gałązka, "Polarimetric investigations of residual stresses in Czochralski-grown $LiNbO_3$ crystals", *Proc. SPIE* **3094**, 147–158 (1996).
16. X. Xu, Z. Zhao, J. Xu, and P. Deng, "Distribution of ytterbium in Yb: YAG crystals and lattice parameters of the crystals", *J. Cryst. Growth* **255**, 338–341 (2003).
17. X. Xu, Z. Zhao, G. Zhao, G. Zhao, P. Song, J. Xu, and P. Deng, "Comparison of Yb:YAG crystals grown by CZ and TGT method", *J. Cryst. Growth* **257**, 297–300 (2003).
18. A. Giesen, U. Brauch, I. Johannsen, M. Karszewski, C. Stewen, and A. Voss, *OSA Trends in Optics and Photonics. Advanced Solid State Lasers*, 11–13 (1996).
19. T. Kasamatsu, H. Sekita, and Y. Kuwano, *OSA Trends in Optics and Photonics. Advanced Solid State Lasers*, 125–127 (1998).

